Distributed Bragg Reflection Dielectric Waveguide Oscillators

BANG-SUP SONG, STUDENT MEMBER, IEEE, AND TATSUO ITOH, SENIOR MEMBER, IEEE

Abstract—**Dielectric waveguide Gunn oscillators are presented in which the cavity consists of grating structures exhibiting either the surface-wave stopband or the leaky-wave stopband. Oscillation conditions and design criteria of the grating structures are studied. When a grating exhibiting the leaky-wave stopband is used in the oscillator, the extraction of the output power in the direction perpendicular to the dielectric waveguide axis is possible. This is because such a grating becomes a broadside-firing leaky-wave antenna with high input VSWR.**

I. Introduction

IN THIS PAPER, we present first a more detailed study of a distributed Bragg reflection (DBR) Gunn oscillator developed earlier [1]. Then we introduce a new DBR oscillator in which a leaky-wave antenna is integrated. These oscillators are made of dielectric waveguides and are believed useful for millimeter and microwave integrated circuits. The leaky-wave antenna integrated in the new structure is broadside firing. In conventional antenna applications, such a broadside condition is avoided due to its high VSWR characteristics. In the present work, however, this high VSWR is intentionally made use of for providing a frequency dependent positive feedback to the gain device in the oscillator.

In most dielectric waveguide millimeter-wave integrated circuits, a solid-state oscillator is made of a Gunn or IMPATT diode implanted in a rectangular dielectric waveguide cavity [2]. In such a structure, the Fresnel reflection from the end surfaces of the resonator provides feedback to the active device and leads to oscillation. In the recently developed original version of the DBR Gunn oscillators [1], however, the feedback is provided by the so-called surface-wave stopband phenomenon of the grating structures created in the dielectric waveguide [3]. As is also demonstrated in the band-reject filter [4], the surface wave is strongly reflected back from the grating structure in a narrow frequency region. Such a frequency sensitive reflection is useful for realizing a high-Q cavity for the oscillator made of a dielectric waveguide. In practice, the DBR oscillator resembles the DBR GaAs lasers developed in optics [5], [6].

It is well known that the stopband phenomenon appears not only in the surface wave, but also in the leaky-wave regions [7]. In the structures described in this paper, the leaky-wave stopband as well as the surface-wave stopband is used for providing positive feedback leading to oscillation. We will test an oscillator in which the grating on one side of the gain device provides a surface-wave stopband and the one on the other side gives a leaky-wave stopband. This leaky-wave structure also gives rise to the broadside radiation which facilitates easy output power extraction.

Manuscript received May 5, 1979; revised September 11, 1979. This work was supported in part by a U.S. Army Research under Grant DAAG29-78-G-0145.

The authors are with the Department of Electrical Engineering, the University of Texas, Austin, TX 78712.

II. Oscillator Design

It is known that Gunn devices exhibit negative differential conductance when the operating frequency is an integral multiple of transit frequency [8], [9]. Therefore, the negative conductance and the positive susceptance of the Gunn device peak around the transit frequency $f_t = \bar{v}/L$, where $\bar{v}$ is the average electron drift velocity and L is the diode length. Since the electron drift velocity depends on the applied field [10], however, it is possible to shift the peak of the negative conductance and the positive susceptance, as well as their amplitudes, by varying the bias voltage until the oscillation conditions in (1a) and (1b) are satisfied. These oscillation conditions are

$$G_d + G_r = 0 \tag{1a}$$

$$B_d + B_r = 0 \tag{1b}$$

where G_d and B_d are the conductance and the susceptance of the diode, and G_r and B_r are the conductance and the susceptance external to the diode. Around the transit frequency, the Gunn device can be represented by an equivalent circuit consisting of a negative conductance ($G_d < 0$) in shunt with a positive susceptance ($B_d > 0$) [11]. Therefore, we have to supply the diode externally with a negative susceptance which is inductive to satisfy the oscillation condition (1b).

Although various types of gratings can be used, mechanically created notch type periodic grooves in the dielectric waveguide have been used in the oscillators. For the surface-wave stopband, the period of grating d is chosen such that

$$\mathrm{Re}(\beta d) = \pi \tag{2}$$

where β is the phase constant of the dielectric waveguide with gratings. β can be approximated by the following dispersion relation [12]:

$$\cos\beta d = \cos(\beta_G a)\cos[\beta_{NG}(d-a)] - \tfrac{1}{2}(\beta_{NG}/\beta_G + \beta_G/\beta_{NG})\sin(\beta_G a)\sin[\beta_{NG}(d-a)] \tag{3}$$

0018-9480/79/1200-1019$00.75 ©1979 IEEE

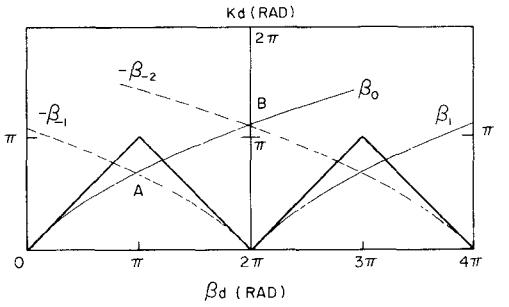

Fig. 1. kd–βd diagram of the grating structure; $\epsilon_r = 10$, $w = 5.6$ mm, $d = 11.0$ mm, $a = 5.5$ mm, $h = 3.0$ mm, $t = 0.9$ mm.

where β_G and β_{NG} are the phase constants in the grooved and nongrooved sections of the waveguide, respectively. In the stopband, β is complex due to mode coupling between the forward and backward waves. When we neglect this mode coupling, the dispersion curve (kd–βd diagram) will look like the one shown in Fig. 1. Point $A(\beta d = \pi)$ corresponds to the surface-wave stopband where strong mode coupling occurs between the two space harmonics β_0 and $-\beta_{-1}$ (negative β means traveling backward). All of these space harmonics are interrelated via

$$\beta_m = \beta_0 + \frac{2m\pi}{d}, \qquad m = 0, 1, 2, \cdots \tag{4}$$

where β_0 is the phase constant of the dominant ($m = 0$) space harmonic.

The leaky-wave stopband is created at $\beta d = 2\pi$ (Point B in Fig. 1) by the interaction between the space harmonics β_0 and $-\beta_{-2}$ which are no longer surface waves, and the radiation peak is in the broadside direction normal to the waveguide surface. This leaky-wave stopband gives strong reflection due to the backward space harmonic $-\beta_{-2}$ being coupled to β_0, which results in high VSWR.

The original version of the DBR oscillator employing a surface-wave stopband can be implemented as in Fig. 2 by placing a Gunn device in a small vertical hole drilled in a dielectric image guide [1]. The ground plane is used as a heat sink as well as a dc bias return for the device. The bias is supplied through a thin wire connected to the positive terminal of the diode. The equivalent circuit of the DBR Gunn oscillator in Fig. 2 can be drawn as in Fig. 3(a) [1], [2], where Y_d is the equivalent admittance of the diode, and Y_1, Y_2 are the input admittances looking into the two grating reflectors on both sides. These grating reflectors are capacitive in the stopband. Thus a quarter-wave transformer is introduced between the diode and the reflector to provide an inductive load to the device. The resulting simplified equivalent circuit is shown in Fig. 3(b) and Fig. 3(c) when we have made use of the following relations:

$$Y_r = Y_0^2\left(\frac{1}{Y_1} + \frac{1}{Y_2}\right) = G_r + jB_r$$

$$Y_d = G_d + jB_d \tag{5}$$

where Y_r is the total equivalent admittance of the externel

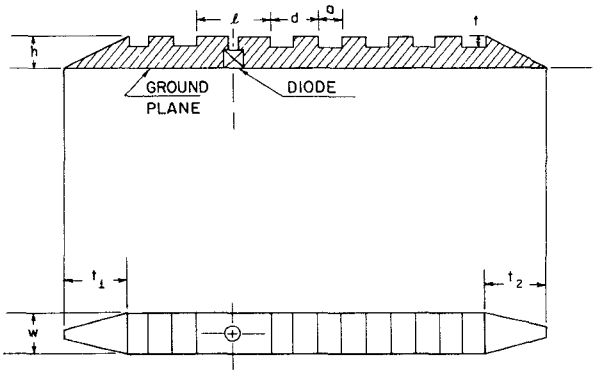

Fig. 2. An original version of the DBR oscillator structure; $\epsilon_r = 10$, $h = 3.0$ mm, $l = 16.5$ mm, $d = 11.0$ mm, $a = 5.5$ mm, $w = 5.6$ mm, $t = 0.9$ mm, $t_1 = 16.0$ mm, $t_2 = 11.5$ mm.

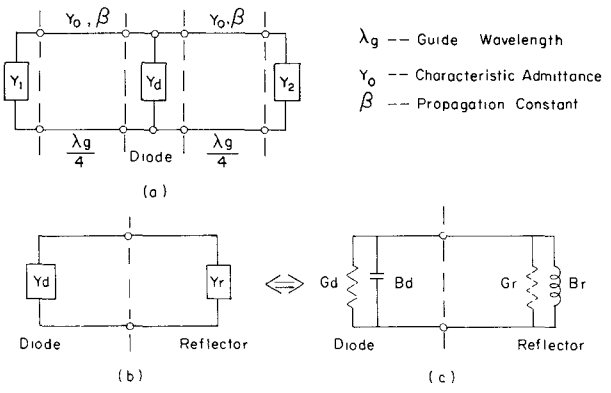

Fig. 3. Equivalent circuit of the DBR oscillator.

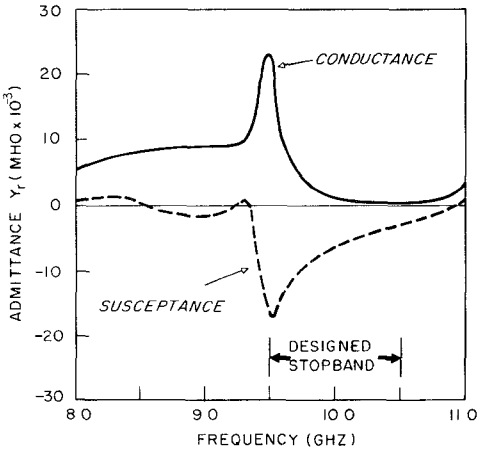

Fig. 4. Admittance external to the diode in the Fig. 2 structure.

reflectors. The variation of Y_r with frequency is shown in Fig. 4 for the DBR oscillator in Fig. 2. The conductance and the susceptance peak at the lower edge of the designed stopband. Even though we cannot determine exactly the values of G_d and B_d of the Gunn device, G_d and B_d can be controlled up to a few millimhos by the externel bias voltage as mentioned earlier in this section. Another important factor which cannot be neglected is the shunt capacitance and the series inductance of the commerical diode packaging which are approximately in the range of a few tenths of a picofarad or nanohenry, respectively. At

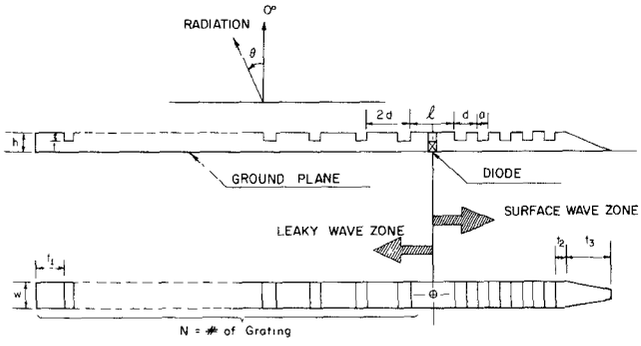

Fig. 5. Structure of a new DBR oscillator with a built-in leaky-wave antenna; $N=10$, $\epsilon_r=10$, $l=22.0$ mm, $d=11.0$ mm, $a=4.0$ mm, $w=6.0$ mm, $t=0.9$ mm, $h=3.0$ mm, $t_1=12.0$ mm, $t_2=4.0$ mm, $t_3=19.0$ mm.

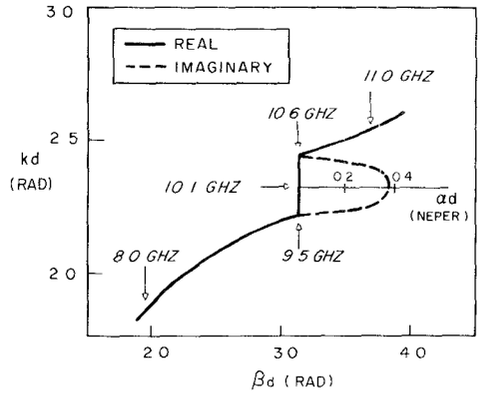

Fig. 6. Detailed kd–βd diagram around the point A in Fig. 1.

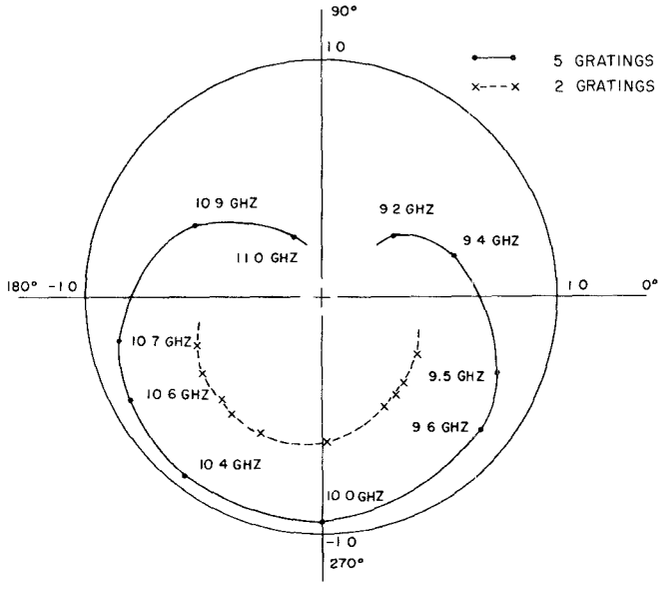

Fig. 7. Reflection coefficient of 5- and 2-element gratings in dielectric waveguide in Fig. 2.

10 GHz, these correspond to 10~40 mho. Therefore, when we consider this effect, oscillations are likely to occur in the lower half of the stopband where the admittance peak is located. So it is better to design the center frequency of the stopband a little higher than the desired operating frequency.

The new DBR oscillator using the high VSWR leaky-wave stopband is shown in Fig. 5. In this structure, the left-hand side of the Gunn diode provides a dual function. It provides the reflection for oscillation as well as the broadside radiation for the antenna. The period of grating on the left is about two times that of the surface-wave structure on the right, viz., $\mathrm{Re}(\beta d)\cong 2\pi$ on the left-hand side and $\mathrm{Re}(\beta d)=\pi$ on the right. The radiation angle from the leaky-wave structure can be determined by [4], [13]

$$\theta=\pm\sin^{-1}\left[\frac{\mathrm{Re}(\beta_{-1})}{k}\right] \tag{6}$$

where θ is the angle measured from the direction normal to the surface and k is the free-space wavenumber. At the leaky-wave stopband (Point B), $\mathrm{Re}(\beta d)\approx 2\pi$ which means a radiation angle of $\theta\approx 0$ (broadside). This angle varies slightly depending on the oscillation frequency.

The reflection phenomenon due to the stopband is frequency sensitive, and the bandwidth and reflection depend on the grating profile, the length of the grating region, etc. In this work, bandwidth has been made wide (1 GHz) so that the oscillation can be easily attained.

III. Results and Discussions

Although we can provide the design at much higher millimeter-wave frequencies, we have selected X band for design and demonstration. This is due to better availability of measurement equipment and greater ease of experimental procedures. After the feasibility of our new concepts is demonstrated, we can go to higher frequencies in the future.

The dielectric waveguides are made of a synthetic dielectric material, Custom HiK ($\epsilon_r=10$). The number of grating elements can be determined by the required magnitude of the feedback. We can calculate the amount of feedback from (3), and the imaginary part of β plotted in Fig. 6 explains the feedback mechanism in the stopband [3], [5], [6]. Fig. 7 shows the surface-wave reflection coefficients of a 5- and 2-element notch-type grating on the dielectric waveguides. Groove depth and grating period are adjusted so as to give a 10-GHz center frequency and a 1-GHz bandwidth. The reflection coefficient at 10 GHz is found to be 0.95 in the 5-element grating, but in the 2-element grating, the reflection coefficient at 10 GHz reduces to 0.63. The latter may be useful for the output port of the original DBR oscillator shown in Fig. 2 in which the far end of each grating is tapered to avoid unwanted end reflection. Even though we design the stopband which spans from 9.5 to 10.5 GHz, oscillation frequencies will be lower than the 10-GHz center frequency as mentioned in Section II. Oscillation frequencies and power output were observed by varying the bias voltage of the Gunn device in the DBR oscillator shown in Figs. 2 and 5. The results are plotted in Figs. 8 and 9. Oscillation frequencies measured were predominantly in the lower half of the stopband (9.5~10.0 GHz). The power was measured by receiving the radiation from one end of the resonator.

In the new DBR oscillator with a built-in leaky-wave antenna, with bias voltage of 7 V, the resonant frequency

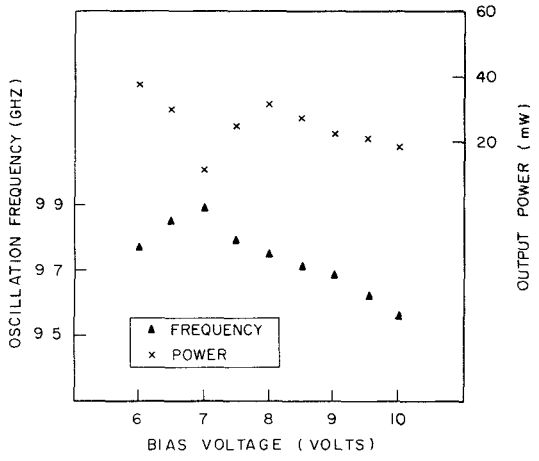

Fig. 8. Measured oscillation characteristics of the oscillator in Fig. 2.

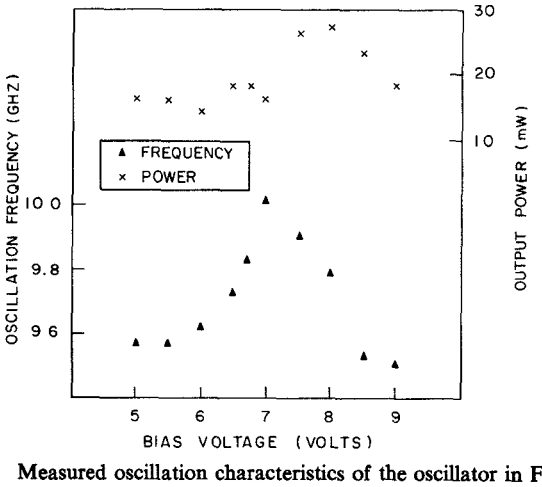

Fig. 9. Measured oscillation characteristics of the oscillator in Fig. 5.

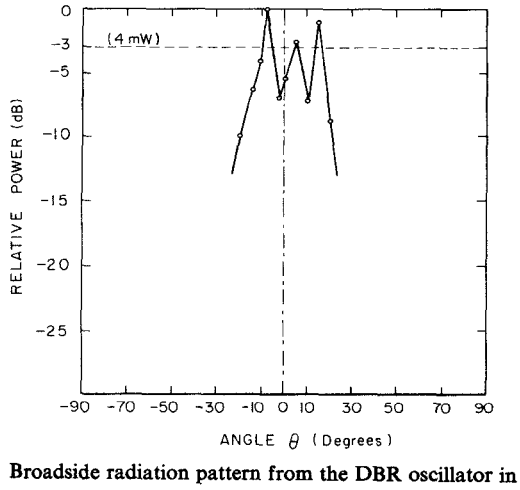

Fig. 10. Broadside radiation pattern from the DBR oscillator in Fig. 5.

was observed around 9.995 GHz, and the measured broadside radiation is shown in Fig. 10. When measuring the radiation pattern, the radiation from the diode was properly shielded.

It is conjectured that the split of the main lobe is caused by several factors. One is the poor spectral purity which is not an inherent phenomenon of this type of oscillator, but is rather due to our intentional broad-band design of the cavity. Another is the strong mode coupling between the forward and backward space harmonics in the leaky-wave region which have different radiation angles.

IV. Conclusions

We have presented studies of DBR Gunn oscillators with surface-wave and leaky-wave stopbands and some results for these oscillator structures. The structure is believed to give versatility in designing millimeter-wave integrated circuits. Further works need to be carried out to obtain spectral purity and better frequency control especially for the structures with an integrated leaky-wave antenna. It is possible to design grating structures with a much narrower bandwidth for more stable oscillation. In designing the oscillator, it is advisable to place the operating frequency in the lower half of the stopband. It is also required to insert quarter-wave transformer between the device and the grating reflector. Mechanical perturbation may be incorporated for adjusting the device impedance for possible tuning of frequency and/or power.

References

[1] T. Itoh and F. Hsu, "Distributed Bragg reflector Gunn oscillators for dielectric millimeter-wave integrated circuits," *IEEE Trans. Microwave Theory Tech.*, vol. MTT-27, pp. 514–518, May 1979.

[2] H. Jacobs, G. Novick, C. M. LoCascio, and M. M. Chrepta, "Measurement of guided wavelength in rectangular dielectric waveguides," *IEEE Trans. Microwave Theory Tech.*, vol. MTT-24, pp. 815–820, Nov. 1976.

[3] S. T. Peng, T. Tamir, and H. L. Bertoni, "Theory of periodic dielectric waveguides," *IEEE Trans. Microwave Theory Tech.*, vol. MTT-23, pp. 123–133, Jan. 1975.

[4] T. Itoh, "Application of gratings in a dielectric waveguide for leaky-wave antennas and band-reject filters," *IEEE Trans. Microwave Theory Tech.*, vol. MTT-25, pp. 1134–1138, Dec. 1977.

[5] S. Wang, "Principles of distributed feedback and distributed Bragg reflection lasers," *IEEE J. Quantum Electron.*, vol. QE-10, pp. 413–427, Apr. 1974.

[6] W. Streifer, D. R. Scifres, and R. D. Burnham, "Coupled wave analysis of DFB and DBR lasers," *IEEE J. Quantum Electron.*, vol. QE-13, pp. 134–141, Apr. 1977.

[7] R. E. Collins, F. J. Zucker, and A. Hessel, *Antenna Theory*. New York: McGraw Hill, 1969, pt. II, ch. 19.

[8] S. M. Sze, *Physics of Semiconductor Devices*. New York: Wiley, 1969, ch. 14.

[9] D. E. McCumber and A. G. Chynoweth, "Theory of negative-conductance amplification and of Gunn Instabilities in two-valley semiconductors," *IEEE Trans. Electron Devices*, vol. ED-13, pp. 4–21, Jan. 1966.

[10] P. N. Robson, G. S. Kino and B. Fay, "Two-Port microwave amplification in long samples of gallium arsenide," *IEEE Trans. Electron Devices*, vol. ED-14, pp. 612–615, Sept. 1967.

[11] H. W. Thim, "Linear microwave amplification with Gunn oscillators," *IEEE Trans. Electron Devices*, vol. ED-14, pp. 517–522, Sept. 1967.

[12] R. E. Collin, *Foundations for Microwave Engineering*, New York: McGraw-Hill, 1966, ch. 8.

[13] K. L. Klohn, R. E. Horn, H. Jacobs and E. Freibergs, "Silicon waveguide frequency scanning linear array antenna," *IEEE Trans. Microwave Theory Tech.*, vol. MTT-26, pp. 764–773, Oct. 1978.